


 Cite this: *RSC Adv.*, 2020, **10**, 43400

Achieving polydispersive HDPE by *N,N,N*-Co precatalysts appended with *N*-2,4-bis(di(4-methoxyphenyl)methyl)-6-methylphenyl†‡

 Shi-Fang Yuan,^{*a} Zhe Fan,^{ab} Yi Yan,^{ab} Yanping Ma,^{id}^{*b} Mingyang Han,^b Tongling Liang,^{id}^b and Wen-Hua Sun,^{id}^{*bc}

A family of unsymmetrical 2-(2,4-bis(di(4-methoxyphenyl)methyl)-6-MeC₆H₂N)-6-(1-(arylimino)ethyl)pyridine-cobalt dichloride complexes has been synthesized and characterized by NMR spectroscopy, FT-IR spectroscopy and elemental analysis as well as single crystal X-ray diffraction for **Co2** and **Co4**. Activated with either MAO or MMAO, all the cobalt precatalysts displayed high activities toward ethylene polymerization and produced highly linear polyethylenes with high molecular weights as well as wide polydispersities; for example, the performance using **Co1**/MAO at 50 °C reached 9.17×10^6 g PE (mol of Co)⁻¹ h⁻¹ with the production polyethylene of molecular weight as high as $M_w = 3.14 \times 10^5$ g mol⁻¹, $T_m = 134.3$ °C besides its wide polydispersity of M_w/M_n of 54.6. Besides the terminal vinyl group of the resultant polyethylenes, it is rare for a late-transition metal catalyst to achieve highly linear polyethylenes with not only wide polydispersity but also high molecular weights, being similar to high-density polyethylenes produced using Phillips catalyst.

 Received 2nd November 2020
 Accepted 23rd November 2020

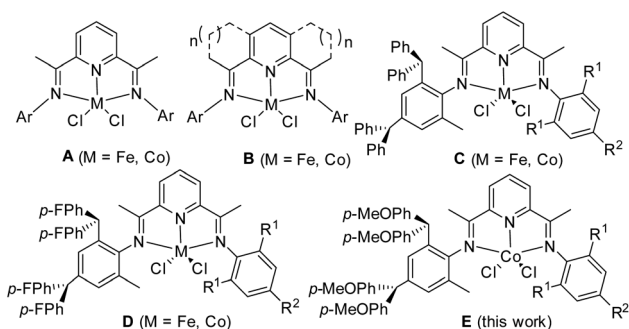
DOI: 10.1039/d0ra09333e

rsc.li/rsc-advances

Introduction

The discovery of bis(imino)pyridine-iron and cobalt dichlorides (**A**, Scheme 1) as highly active precatalysts for ethylene polymerization heralded a new era in the organometallic application of late transition metals as well as polyolefin catalysts.¹ Subsequently, many researchers from both academia and industry have developed various ligand units through extensive modification of 2,6-bis(imino)pyridine derivatives² and newly designed *N*-heterocyclic compounds such as 2-benzimidazolyl-6-aryliminopyridines,³ *N*-[(pyridin-2-yl)methylene]-8-arylaminopyridines,⁴ 2,8-bis(arylimino)-quinolones,⁵ and 2-arylimino-1,10-phenanthrolines,⁶ which have appeared as compatible supports for cobalt and iron precatalysts.^{2,7} More importantly the incorporation of fused carbocyclic rings to the central pyridine (**B**, Scheme 1) has been systematically implemented

leading to novel ligands containing either singly or doubly fused derivatives with ring sizes of between five and eight for introducing controlled amounts of strain to the parent bis(imino)pyridine framework with a view to modifying the donor properties of the tridentate ligands.^{8,9} With the particular regard to cobalt precatalysts, polyethylenes with different molecular weights were produced by those catalytic systems;⁹ for examples, precatalysts supported by the single five-membered fused^{9a} or doubly six-membered fused systems^{9b} produced from oligomers to polyethylene. Narrow dispersive polyethylenes were formed by precatalysts with the single six-,^{9c} or seven-numbered fused systems^{9d} as well as doubly seven-^{9e} or eight-membered fused systems;^{9f} in addition, polyethylenes



Scheme 1 Structural variations in bis(imino)pyridine-cobalt and -iron precatalysts (A–E).

^aInstitute of Applied Chemistry, Shanxi University, Taiyuan 030006, People's Republic of China. E-mail: yuansf@sxu.edu.cn

^bKey Laboratory of Engineering Plastics, Beijing National Laboratory for Molecular Sciences, Institute of Chemistry Chinese Academy of Sciences, Beijing 100190, China. E-mail: whsun@iccas.ac.cn; Fax: +86-10-62618239; Tel: +86-10-62557955

^cState Key Laboratory for Oxo Synthesis and Selective Oxidation, Lanzhou Institute of Chemical Physics, Chinese Academy of Sciences, Lanzhou 730000, China

† Dedicated to Prof. Dr Sabu Thomas on his 60th birthday.

‡ Electronic supplementary information (ESI) available: NMR charts of cobalt complexes and representative polymeric samples as well as crystal data and structure refinements for **Co2** and **Co4**. CCDC 2027357 (**Co2**) and 2027358 (**Co4**). For ESI and crystallographic data in CIF or other electronic format see DOI: 10.1039/d0ra09333e



with mono- to bimodal distributions were achieved through using different cocatalysts.^{9f}

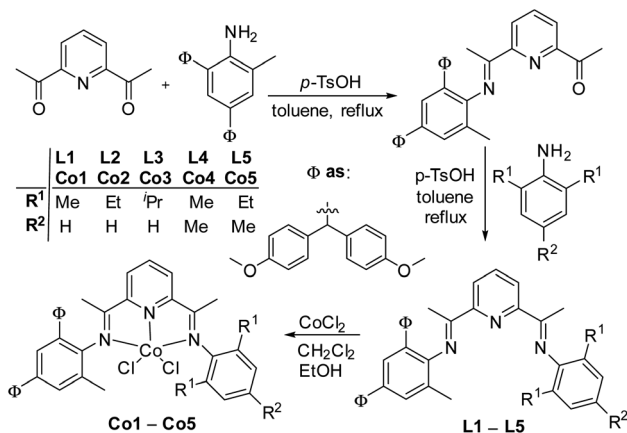
From industrial view, the investigation is worthily conducted not for the precatalysts themselves, but for the polyethylenes formed and their properties demanded. Though there is critical comment on the trace toxic chromium remained in the resultant polyethylenes by Phillips catalysts, the obtained polyethylenes provide better performances of “shear thinning” and “melt strength” because of their unique wide polydispersities (8–65).¹⁰ With this fact in mind, the bis(arylimino)pyridylcobalt model¹ is reconsidered for its possibility for polydispersive polyethylenes; that is, the cobalt catalytic system is also worthily explored in producing polyethylenes with wide dispersity instead of narrow dispersive polyethylenes being pursued.²

The *N*-aryl groups diversification of bis(arylimino)pyridines has finely turned their cobalt complex precatalysts for varying catalytic performances and obtaining polyethylenes with different properties;^{2a,7b} especially, the promising precatalysts of iron or cobalt complexes have been developed through using benzhydryl substituents^{11,12} either benzhydryl^{6,11,12a} or its derivative di(4-fluorophenyl)methyl.^{12b} Within these precatalysts, higher catalytic activities have been commonly achieved when using unsymmetric phenylamine derivatives such as **C** (Scheme 1) from 2,4-dibenzhydryl-6-methylphenylamine^{12c,d} and **D** (Scheme 1) from 2,4-bis(di(4-fluorophenyl)-methyl)-6-methylphenylamine,^{12e} and the latter exhibited good thermal stability. Subsequently the methoxy group was introduced into the benzhydryl group, producing the unsymmetric 2-(2,4-bis(di(4-methoxyphenyl)-methyl)-6-MeC₆H₂N)-6-(1-(arylimino)ethyl)pyridine cobalt(II)chlorides (**E**, Scheme 1), of which the catalytic performance was investigated towards ethylene polymerization. Interestingly, the resultant polyethylenes are significantly different to those obtained by previously cobalt precatalysts; the polydispersive, high molecular weight and linear polyethylenes are firstly achieved by cobalt complex precatalysts. These may result a potential of industrial application. Herein the synthesis and characterization of the title cobalt complexes were described as well as their catalytic performances under various polymerization conditions along with microstructures of resultant polymers.

Results and discussion

Synthesis and characterization of the cobalt(II) complexes Co1–Co5

The compound 2,4-bis(di(4-methoxyphenyl)methyl)-6-methylaniline was synthesized using the similar procedure reported previously,¹³ which reacts with 2,6-diacetylpyridine to prepare monoketone derivative, 2-acetyl-6-(1-(2,4-bis(di(4-methoxyphenyl)methyl)-6-methylphenylimino)ethyl)pyridine. Then refluxing the monoketone derivative and equivalent aniline with a catalytic amount of *p*-TsOH in toluene formed a series of 2-(1-(2,4-bis(di(4-methoxyphenyl)methyl)-6-methylphenylimino)ethyl)-6-(1-(arylimino)ethyl)pyridine ligands (**L1**–**L5**) in acceptable yields {aryl = 2,6-Me₂C₆H₃ (**L1**), 2,6-Et₂C₆H₃ (**L2**), 2,6-ⁱPr₂C₆H₃ (**L3**), 2,4,6-Me₃C₆H₂ (**L4**) and 2,6-Et₂-4-



Scheme 2 Synthetic procedure for the ligands **L1**–**L5** and their cobalt complexes **Co1**–**Co5**.

MeC₆H₂ (**L5**)} (Scheme 2). All the organic compounds were fully characterized by ¹H and ¹³C NMR spectroscopy, elemental analysis, and the FT-IR spectra. The organic compounds reacted with cobalt dichlorides in dichloromethane and ethanol to form their corresponding cobalt complexes **Co1**–**Co5** (Scheme 2) in good yields, brown solids. All new cobalt complexes have been characterized by elemental analysis as well as ¹H NMR, and FT-IR spectroscopy. In the FT-IR spectra, the stretching vibrations for C=N_{imine} bonds in the complexes appear in the range of 1615–1627 cm⁻¹ which are lower in wave number than those for the free ligands (1643–1650 cm⁻¹), indicating the coordination of the ligand with the cobalt metal atom. Such shifts are consistent with structurally related cobaltous chloride complexes reported elsewhere.^{12,14b}

Moreover, in the ¹H NMR spectra of **Co1**–**Co5**, recorded in CDCl₃ at ambient temperature, broad paramagnetically shifted peaks are a feature of all the complexes (Fig. 1 and S1–S4[†]). The assignment of the peaks has been made through a comparison with data recorded for related Co(II) (*S* = 3/2) complexes, relative

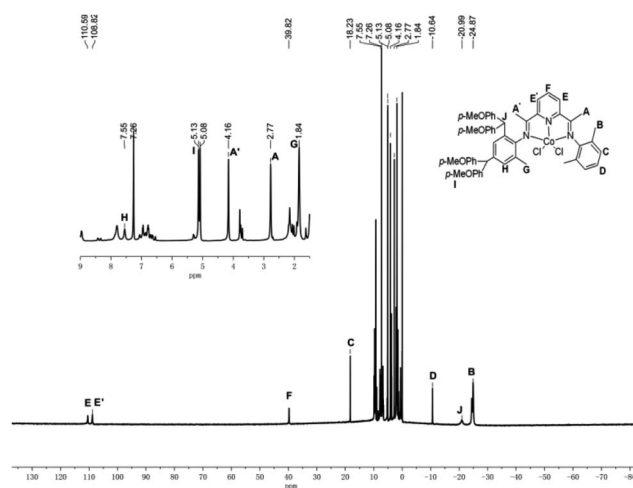


Fig. 1 ¹H NMR spectrum of **Co1**; recorded in CDCl₃ at ambient temperature.



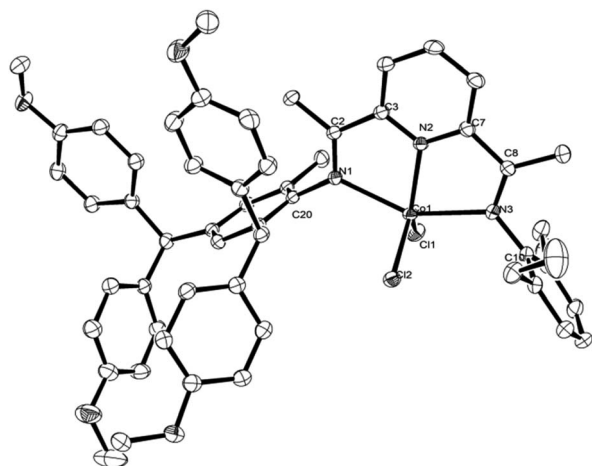


Fig. 2 Molecular structure of complex **Co2** with thermal ellipsoids at 30% probability. Hydrogen atoms have been omitted for clarity.

integration and proximity to the paramagnetic center.^{1c,2b,14} Taking the complex **Co1** for example, two downfield peaks at δ 39.82 (F) and δ 110.59/108.82 (E/E') can be assigned to the *para*-pyridyl and *meta*-pyridyl protons, respectively, which is consistent with data reported elsewhere. On the other hand, the non-equivalent *meta*-aryl protons can be seen more upfield at δ 7.55 (H for Ar-Hm) and δ 18.23 (C for Ar-Hm) (Fig. 1). As previously mentioned,^{14b} the more upfield peaks can be assigned to the methyl protons B (δ -24.87), and the CH(*p*-MeOC₆H₄)₂ protons have been ascribed to the signal at δ -20.99.

To further confirm the structural identity of the complexes, **Co2** and **Co4** were used for representative examples as single crystal X-ray diffraction studies. Single crystals of **Co2** and **Co4** were grown by slow diffusion of hexane into a dichloromethane solution. Their molecular structures are shown in Fig. 2 and 3; selected bond lengths and angles are listed in Table 1. The structures of **Co2** and **Co4** are analogous to each other.

As shown in Fig. 2 and 3, in each case a single cobalt center is bound by two chloride ligands and three nitrogen donors, N1,

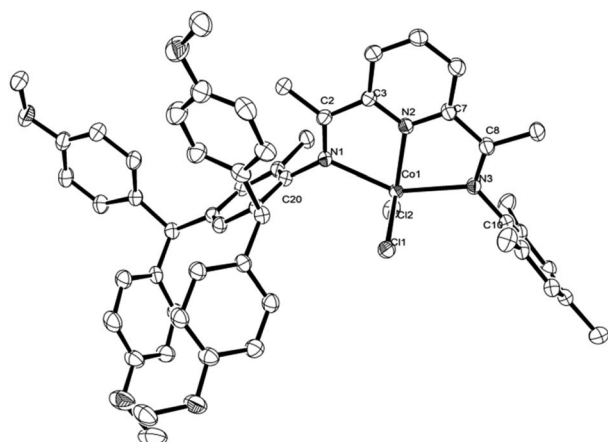


Fig. 3 Molecular structure of complex **Co4** with thermal ellipsoids at 30% probability. Hydrogen atoms have been omitted for clarity.

Table 1 Selected bond lengths (Å) and angles (°) for **Co2** and **Co4**. Catalytic performance for ethylene polymerization

	Co2	Co4
Bond lengths (Å)		
Co(1)–N(1)	2.266(2)	2.286(2)
Co(1)–N(2)	2.030(2)	2.041(2)
Co(1)–N(3)	2.274(2)	2.282(2)
Co(1)–Cl(1)	2.2529(8)	2.2372(7)
Co(1)–Cl(2)	2.2484(8)	2.2352(8)
N(1)–C(2)	1.281(3)	1.280(4)
N(1)–C(20)	1.441(3)	1.442(3)
N(2)–C(3)	1.341(3)	1.342(3)
N(2)–C(7)	1.343(3)	1.335(3)
N(3)–C(8)	1.277(4)	1.284(4)
N(3)–C(10)	1.441(3)	1.434(4)
Bond angles (°)		
N(1)–Co(1)–N(2)	75.55(8)	74.98(8)
N(1)–Co(1)–N(3)	150.47(8)	149.94(8)
N(1)–Co(1)–Cl(1)	95.35(6)	100.65(6)
N(1)–Co(1)–Cl(2)	100.78(6)	93.68(6)
N(2)–Co(1)–N(3)	74.97(8)	74.96(8)
N(2)–Co(1)–Cl(1)	124.09(7)	117.13(7)
N(2)–Co(1)–Cl(2)	120.99(7)	126.71(7)
N(3)–Co(1)–Cl(1)	102.44(7)	93.03(6)
N(3)–Co(1)–Cl(2)	92.90(6)	104.17(6)
C(10)–N(3)–Co(1)	124.78(17)	125.96(17)
C(20)–N(1)–Co(1)	128.15(16)	126.27(16)

N2 and N3, to afford a distorted square pyramidal geometry; structurally related five-coordinate species have been previously reported.¹² The cobalt atom lies 0.046 Å above the basal plane for **Co2** and 0.002 Å for **Co4**. The Co(1)–N(2) pyridine bond [2.030(2) Å, **Co2**, and 2.041(2) Å, **Co4**] is significantly shorter than the Co(1)–N(1) imine and Co(1)–N(3) imine bonds [2.266(2) and 2.274(2) Å, **Co2**, 2.286(2) and 2.282(2) Å, **Co4**], indicating stronger coordination of *N*-pyridine with a metal center. The *N*-aryl groups are nearly right angled with respect to the plane of the N¹N²N³ chelate dihedral angle: 82.9° and 83.5° for **Co2** and 85.8° and 79.2° for **Co4**, revealing the potential catalytic ability in ethylene polymerization.

To develop the potential of precatalysts **Co1**–**Co5** to reconcile the polymerization of ethylene, methylaluminoxane (MAO) and modified methylaluminoxane (MMAO) were chosen as activator, both aluminoxanes have a reputation for being among the most potent in cobalt polymerization catalysis.^{12,15} The Al/Co molar ratio, reaction temperature, run time and ethylene pressure are all parameters to be investigated. The molecular weights (M_w) and molecular weight distributions (M_w/M_n) of the resultant polyethylenes were determined by gel permeation chromatography (GPC), while their melt temperatures (T_m) were determined by differential scanning calorimetry (DSC). In all cases gas chromatography (GC) was used to detect for any oligomeric fractions. In addition, the structural properties of selected samples of polyethylene were investigated using ¹H/¹³C NMR spectroscopy.



Table 2 Ethylene polymerization results using Co1/MAO^a

Entry	Precat.	Al/Co	T (°C)	t (min)	Yield (g)	Activity ^b	M _w	M _w /M _n ^c	T _m ^d (°C)
1	Co1	2500	30	30	0.38	0.51	3.45	36.2	136.2
2	Co1	2500	40	30	0.94	1.25	3.40	62.0	136.1
3	Co1	2500	50	30	2.87	3.83	3.32	35.9	135.5
4	Co1	2500	60	30	0.84	1.12	3.31	57.2	135.2
5	Co1	3000	50	30	5.82	7.76	3.22	56.0	135.1
6	Co1	3250	50	30	6.88	9.17	3.14	54.6	134.3
7	Co1	3500	50	30	6.74	8.99	2.96	55.4	133.7
8	Co1	3750	50	30	6.43	8.57	2.89	52.3	133.8
9	Co1	4000	50	30	6.08	8.11	2.24	22.9	135.0
10	Co1	3250	50	5	4.71	37.68	2.87	43.2	133.3
11	Co1	3250	50	15	5.52	14.72	3.01	57.7	134.2
12	Co1	3250	50	45	7.46	6.63	3.36	56.3	134.5
13	Co1	3250	50	60	7.83	5.22	3.47	58.6	134.2
14 ^e	Co1	3250	50	30	3.19	4.25	2.75	53.5	134.6
15 ^f	Co1	3250	50	30	0.43	0.57	1.86	36.3	135.4

^a Conditions: 1.5 μmol of Co1; 100 mL toluene, 10 atm ethylene. ^b Values in units of 10⁶ g PE (mol of Co)⁻¹ h⁻¹. ^c Determined by GPC, and M_w: 10⁵ g mol⁻¹. ^d Determined by DSC. ^e 5 atm of ethylene. ^f 1 atm of ethylene.

Ethylene polymerization with the Co1/MAO

In the first instance Co1 was employed as the test precatalyst in combination with MAO as a means to ascertain the optimum set of operating conditions, the results are tabulated in Table 2. With the ethylene pressure at 10 atm and the Al/Co ratio at 2500, the temperature was altered from 30 °C to 60 °C (entries 1–4, Table 2), over a thirty-minute run time. A supreme value of the catalytic activity of 3.83 × 10⁶ g PE (mol of Co)⁻¹ h⁻¹ was observed at 50 °C (entry 3, Table 2) affording polymers; no trace of short chain oligomers could be detected, which is outstanding to compare with the activity of the catalyst at other temperatures. As preliminary reported, cobalt catalysts tend to be quite sensitive towards reaction temperature.^{5,11a,d} The polymers showed high molecular weight falling in the scope of 3.45 to 3.31 × 10⁵ g mol⁻¹, which are shown by the GPC curves in Fig. 4. The molecular weights of the polymers gradually decrease on increasing temperature, which can be accredited to a higher rate of chain transfer relative to chain propagation at elevated temperature.¹¹

Subsequently, the influence of Al/Co molar ratio was investigated with the reaction temperature fixed at 50 °C. On elevating the Al/Co molar ratio from 2500 to 4000 (entries 3 and 5–9, Table 2), the highest activity (9.17 × 10⁶ g PE (mol of Co)⁻¹ h⁻¹) was revealed at an Al/Co molar ratio of 3250 (entry 6, Table 2). And the molecular weights of the polyethylene were high (range: 3.4 × 10⁵ g mol⁻¹ to 2.24 × 10⁵ g mol⁻¹) and decreased as the Al/Co molar ratio increased (Fig. 5). This latter observation can be credited to promoting chain transfer from cobalt to aluminum by increasing the amount of alkyl aluminum reagent.^{9e,16} Surprisingly, the dispersities for the resultant polyethylene are particular high, in the range 22.9–62.0, indicating multi-site behaviour for the active species. In previous literature,^{8f,15} resultant polyethylenes showed wide molecular weight distributions, however, some portion were quite low molecular weights. In addition, the quenched filtrates of current catalytic system were carefully examined by GC without observing any low-molecular polymers solved. Therefore the resultant polyethylenes by the title cobalt precatalysts could be

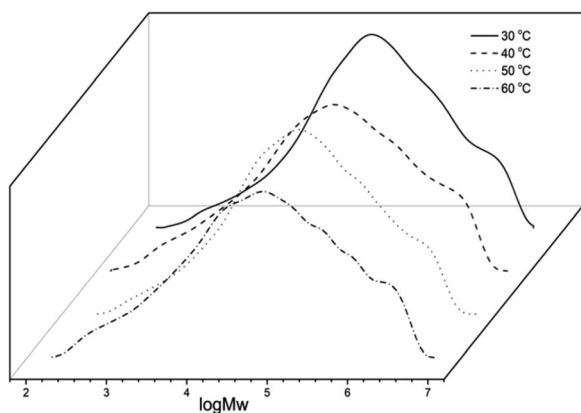


Fig. 4 GPC curves of the polyethylenes (entries 1–4, Table 2).

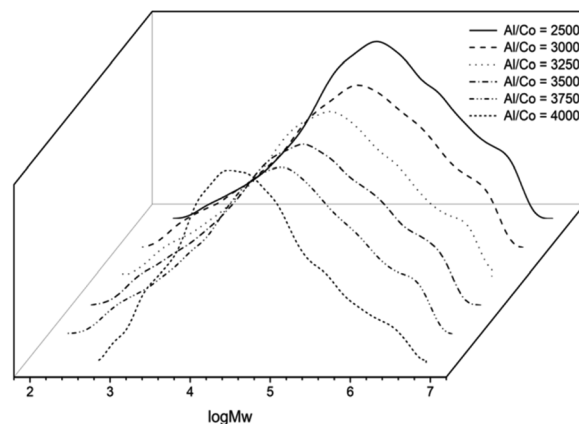


Fig. 5 GPC curves of the polyethylenes (entries 3 and 5–9, Table 2).



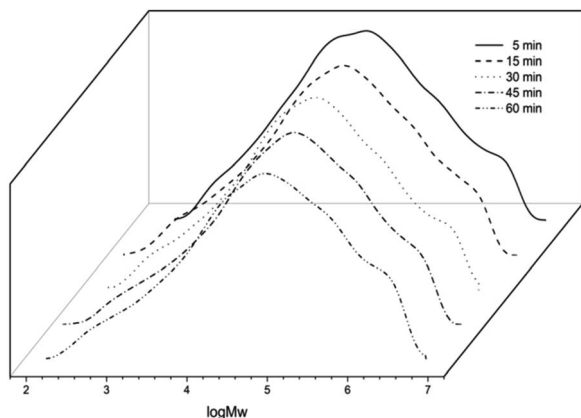


Fig. 6 GPC curves of the polyethylenes (entries 6 and 10–13, Table 2).

expected to be alert polymers used with the properties of those by Phillips catalyst.¹⁰

To explore the lifetime of the active species derived from **Co1**/MAO, the polymerization runs were conducted over 5, 15, 30, 45, and 60 minutes (entries 6 and 10–13, Table 2) with the Al/Co ratio at 3250 and the temperature at 50 °C. The maximum activity of 37.68×10^6 g PE (mol of Co)⁻¹ h⁻¹ was observed after 5 min (entry 10, Table 2), which indicated the active species was rapidly generated after MAO addition and the catalytic process has barely induction period. Meanwhile, their activities gradually decreased along with prolonging reaction time from 5 to 60 min (Fig. 6), it is line with previous reports.^{1b,11d} Furthermore, ethylene pressure (10 atm, 5 atm, 1 atm) was investigated, the activity dramatically dropped from 9.17×10^6 g PE (mol of Co)⁻¹ h⁻¹ to 0.57×10^6 g PE (mol of Co)⁻¹ h⁻¹ (entries 6, 14 and 15, Table 2) which can be accounted for, in part, to mass transport limitations of the monomer at this low pressure. Likewise, the molecular weights decreased with a reducing in ethylene pressure, in agreement with less facile insertion and lower solubility of the ethylene in the reaction solution at lower ethylene pressure.^{11d,18}

Ethylene polymerization with the Co1–Co5/MAO

In order to investigate the influence of the ligand structure on the catalytic behavior, **Co2**–**Co5** were additionally screened for ethylene polymerization under the optimum catalytic

Table 3 Ethylene polymerization results using Co1–Co5/MAO under optimized conditions^a

Entry	Precat.	Yield (g)	Activity ^b	M_w^c	M_w/M_n^c	T_m^d (°C)
1	Co1	6.88	9.17	3.14	54.6	134.3
2	Co2	6.51	8.68	3.92	41.0	135.4
3	Co3	4.07	5.43	4.00	31.9	136.7
4	Co4	6.99	9.32	2.74	46.5	134.7
5	Co5	6.75	9.00	4.33	47.5	135.5

^a Conditions: 1.5 μmol of Co; 100 mL toluene, 10 atm ethylene. ^b Values in units of 10^6 g PE (mol of Co)⁻¹ h⁻¹. ^c Determined by GPC, and M_w : 10^5 g mol⁻¹. ^d Determined by DSC.

conditions (Al/Co ratio = 3250, 10 atm C₂H₄, 50 °C, 30 min) established independently for **Co1**/MAO. On activation with MAO, **Co1**–**Co5** displayed good activities [5.43 – 9.32×10^6 g PE (mol of Co)⁻¹ h⁻¹], falling in the order **Co4** [2,6-di(Me)] > **Co1** [2,4,6-tri(Me)] > **Co5** [2,6-di(Et)-4Me] > **Co2** [2,6-di(Et)] > **Co3** [2,6-di(i-Pr)] (entries 1–5, Table 3). As indicated in the Fig. 7, the activities of **Co4** and **Co5** with methyl group in the *para* position, were higher than the *para*-hydrogen complexes, **Co1** and **Co2**, highlighting a positive effect of having an electron donating methyl group on the catalytic activity. **Co3** owned the lowest activity because of the largest steric hindrance. With regard to the molecular weight, the polyethylenes display values ranging from 2.74×10^5 g mol⁻¹ to 4.33×10^5 g mol⁻¹ with **Co5** [2,6-di(Et)-4-Me] exhibiting the highest value (entry 5, Table 3), which revealed that the particular steric properties in **Co5**/MAO are most suitable to promote chain growth leading to polyethylenes with relatively high molecular weights.^{3a,11a} Furthermore, all polyethylenes obtained by **Co1**–**Co5** exhibited wide molecular weight distribution (PDI = 31.9–54.6).

Ethylene polymerization with the Co1/MMAO

With the ethylene pressure fixed at 10 atm, **Co1**/MMAO was again optimized by varying the Al/Co ratio, reaction temperature and reaction time, the results are collected in Table 4. In comparison with the **Co1**/MAO system, the **Co1**/MMAO system also revealed best activity at 50 °C (entries 1–6, Table 4) affording a polymeric product, no trace of short chain oligomers could be detected. With the increase of temperature, the activity decreases continuously, but up to 80 °C, the activity can still reach 2.79×10^6 g PE (mol of Co)⁻¹ h⁻¹, which proves the good thermal stability of the **Co1**/MMAO system. Then, the molecular weight of the polymer has a significant trend of decrease with the increase of temperature, which is consistent with previous reports.^{9,11} The GPC curves for them in Fig. S5.† Similarly, a wide molecular weight distribution of polyethylene (PDI = 20.7–28.4) was obtained, suggesting multi-active sites.^{11d}

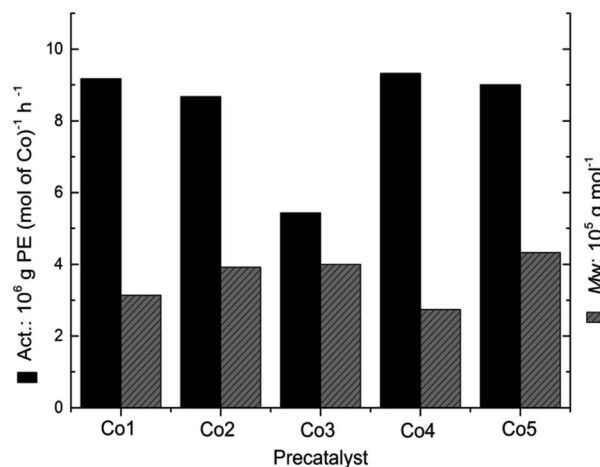


Fig. 7 Comparative activity of Co1–Co5 and the M_w of the corresponding polymers (entries 1–5, Table 3).



Table 4 Ethylene polymerization results using Co1/MMAO^a

Entry	Precat.	Al/Co	<i>T</i> (°C)	<i>t</i> (min)	Yield (g)	Activity ^b	<i>M_w</i> ^c	<i>M_w</i> / <i>M_n</i> ^{b,c}	<i>T_m</i> ^d (°C)
1	Co1	2500	30	30	4.09	5.45	2.04	28.4	135.7
2	Co1	2500	40	30	4.32	5.76	1.54	23.9	135.9
3	Co1	2500	50	30	4.76	6.35	1.50	20.7	135.4
4	Co1	2500	60	30	4.28	5.71	1.04	25.8	133.6
5	Co1	2500	70	30	3.88	5.17	0.96	23.2	133.4
6	Co1	2500	80	30	2.09	2.79	0.93	26.6	130.1
7	Co1	2000	50	30	3.92	5.23	1.71	29.9	134.4
8	Co1	2750	50	30	5.25	7.00	1.43	26.0	134.3
9	Co1	3000	50	30	4.67	6.23	1.22	25.3	134.4
10	Co1	3250	50	30	4.18	5.57	1.08	25.5	133.9
11	Co1	3500	50	30	4.08	5.44	1.00	22.2	135.3
12	Co1	2750	50	5	1.76	14.08	1.12	24.5	134.7
13	Co1	2750	50	15	3.54	13.29	1.39	33.8	134.0
14	Co1	2750	50	45	5.49	4.88	1.58	31.6	134.4
15	Co1	2750	50	60	5.60	3.73	1.79	32.7	135.6
16 ^e	Co1	2750	50	30	2.80	3.73	0.99	21.1	133.3
17 ^f	Co1	2750	50	30	0.68	0.19	0.18	5.97	129.9

^a Conditions: 1.5 μmol of Co1; 100 mL toluene, 10 atm ethylene. ^b Values in units of 10⁶ g PE (mol of Co)⁻¹ h⁻¹. ^c Determined by GPC, and *M_w*: 10⁵ g mol⁻¹. ^d Determined by DSC. ^e 5 atm of ethylene. ^f 1 atm of ethylene.

Further investigations were performed by varying the Al/Co ratio from 2000 to 3500 at a fixed temperature of 50 °C (entries 3 and 7–11, Table 4). Inspection of the polymerization data revealed that the highest activity (7.00 × 10⁶ g PE (mol of Co)⁻¹ h⁻¹) was gained with an Al/Co ratio of 2750 (entry 8, Table 4). Below or above this Al/Co ratio there were negative effects on the activities.^{8,9} The molecular weights of polymers steadily decreased from 1.71 to 1.00 × 10⁵ g mol⁻¹ with the increase in Al/Co ratio (Fig. S6†).

The catalytic activity is inversely related to the polymerization time, and the highest value of 14.08 × 10⁶ g PE (mol of Co)⁻¹ h⁻¹ was found at 5 min run time, indicating a short induction time required to generate the active sites (entry 12, Table 4). With the prolonged reaction time the activity gradually decreases (entries 8 and 13–15 Table 4) and the moderate value of 3.73 × 10⁶ g PE (mol of Co)⁻¹ h⁻¹ was found even for 60 min (Table 4, entry 15), suggesting rather long lifetime of the active sites. The molecular weight of the obtained polyethylene increases constantly with reaction time. The product exhibits unimodal molecular weight distribution and the GPC curve of the reaction time is given in Fig. S7.† Similar dependencies have been observed for the related catalytic systems.^{12a,19} Furthermore, on reducing the pressure from 10 to 1 atm C₂H₄ the molecular weight of the polymer formed using Co1/MMAO significantly dropped (entries 8 and 17 Table 4), while at 5 atm C₂H₄ the molecular weight was as expected between that observed at the two limiting pressures (entries 8, 16 and 17, Table 4). Likewise the catalytic activity showed a similar downward trend as the ethylene pressure was decreased with value at 5 atm about half of that achieved at 10 atm.

Ethylene polymerization with the Co1–Co5/MMAO

Similarly, Co2–Co5/MMAO were screened using the optimum polymerization conditions (Al/Co ratio = 2750, 10 atm C₂H₄,

50 °C, 30 min) established independently for Co1/MMAO. In this case, Co1–Co5/MMAO displayed a narrower range in catalytic activities (3.59–7.00 × 10⁶ g PE (mol of Co)⁻¹ h⁻¹) that falls in the order: Co1 > Co4 > Co2 > Co5 > Co3 (entries 1–5, Table 5, Fig. S8†). Different to that in MAO (Co4 as the highest), Co1 exhibited the highest activity in MMAO and then drops as the steric properties of the *ortho*-positions of the *N*-aryl group progressively increase; this finding can be attributed to the relative ease of ethylene coordination at the active site.^{9f,11d}

Interestingly, Co4 and Co5 with an additional methyl group exhibited a lower activity than that displayed with Co1 and Co2, which suggests a detrimental effect on catalyst performance by an electron donating group in this system, which is contrast to those in MAO.^{12a,b} In terms of the molecular weight of the polymer, this was found to range from 1.03 to 1.87 × 10⁶ g PE (mol of Co)⁻¹ h⁻¹ which is appreciably lower than with Co/MAO, the polymer formed using Co3 [2,6-di(*i*-Pr)] displayed the highest molecular weight 1.87 × 10⁵ g mol⁻¹, this showed that the steric hindrance within Co3 continuously enhanced chain-

Table 5 Ethylene polymerization using Co1–Co5/MMAO under optimized conditions^a

Entry	Precat.	Yield (g)	Activity ^b	<i>M_w</i> ^c	<i>M_w</i> / <i>M_n</i> ^c	<i>T_m</i> ^d (°C)
1	Co1	5.25	7.00	1.43	26.0	134.3
2	Co2	4.51	6.01	1.33	18.7	135.0
3	Co3	2.69	3.59	1.87	16.3	136.1
4	Co4	4.99	6.65	1.03	20.7	133.9
5	Co5	4.38	5.84	1.53	16.6	135.2

^a Conditions: 1.5 μmol of Co; 100 mL toluene, 10 atm ethylene. ^b Values in units of 10⁶ g PE (mol of Co)⁻¹ h⁻¹. ^c Determined by GPC, and *M_w*: 10⁵ g mol⁻¹. ^d Determined by DSC.



growth leading to polyethylenes with relatively high molecular weights.^{9e,14b}

In most of the cases, the melting points of the resultant polyethylenes were higher than 130 °C, which suggests highly linear structures. To further investigate the microstructural properties of the polyethylenes, polyethylene obtained with **Co1**/MAO at 50 °C (entry 6, Table 2) and **Co1**/MMAO at 50 °C (entry 8, Table 4) were characterized by high-temperature ¹H NMR and ¹³C NMR measurements at 100 °C in deuterated 1,1,2,2-tetra-chloroethane-*d*₂. As shown in Fig. 8, polyethylene obtained with **Co1**/MAO at 50 °C display multiplet at $\delta = 5.91$ ppm (a) and $\delta = 5.03$ ppm (b) in the ¹H NMR spectrum, together with the peaks around $\delta = 114.4$ (a) and 139.6 ppm (b) in the ¹³C NMR spectrum, indicating that vinyl groups (–CH=CH₂) were formed through the process of β -hydride elimination as a termination reaction. The high intensity of the singlet at $\delta = 1.36$ ppm in the ¹H NMR spectrum and the single peak of high intensity around $\delta = 30$ ppm in the ¹³C NMR spectrum confirm the high linearity polyethylenes obtained. The carbon atoms of the methyl group at the saturated end of the macromolecule were observed at 14.26 ppm (e), along with the carbon atoms located at the close vicinity (c, d, and f) at 33.99, 32.23 and 22.92 ppm, respectively in Fig. 8.^{20c} Meanwhile, as illustrated in the Fig. S9,[†] ¹H NMR and ¹³C NMR spectra of polyethylene obtained with **Co1**/MMAO were similar to those obtained with **Co1**/MAO at 50 °C, indicating the vinyl groups (–CH=CH₂) were also formed in the process of polymerization by **Co1**/MMAO at 50 °C.

To compare the catalytic performance of cobalt precatalysts with the methoxy in the benzhydryl group in this work with those with other groups (C and D in Scheme 1), the molecular weights and activities for the pre-catalysts C and D are displayed with current pre-catalyst E (**Co1**/MAO) together in Fig. 9.^{12c,e} All three pre-catalysts like **Co1**/MAO [2,6-di(Me)] were screened under optimized conditions. Compared with C and D, the catalytic activity of E is slightly reduced, but the molecular weight of the polymer produced by E is much higher than that

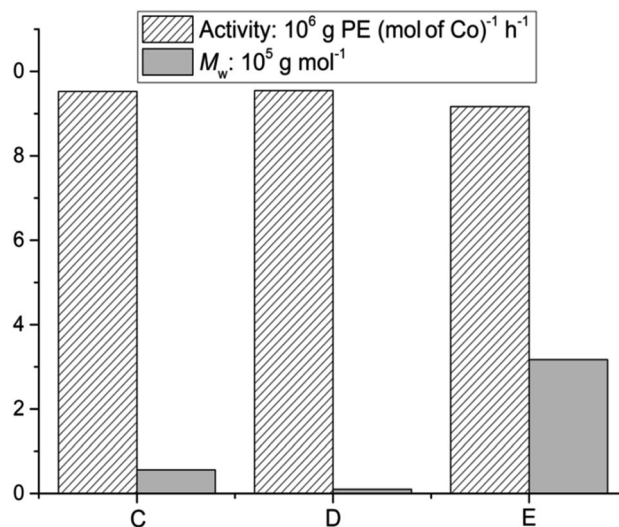


Fig. 9 Comparison of the catalytic performance of **Co1**/MAO with previously reported comparators C and D (Scheme 1).

of C and D, so it can be seen that the introduction of methoxy group plays a positive role in the molecular weight of the polymer. The polyethylenes by C or D exhibits narrow molecular weight distribution range from 1.8 to 3.5,¹² however, polymers by E show broad polydispersities from 22.9 to 62.0, confirming multiple active sites in catalytic system of E besides its continuous growth for the resultant polyethylenes with high molecular weights.

Experimental

General considerations

All operations including air and/or moisture sensitive compounds were performed under an atmosphere of nitrogen using standard Schlenk techniques. All solvents were dried over sodium and distilled under nitrogen atmosphere prior to use. Methylaluminoxane (MAO, 1.46 M in toluene) and modified methylaluminoxane (MMAO, 1.93 M in heptane) were purchased from Albemarle Corporation. Polymer grade of ethylene was purchased from Beijing Yanshan Petrochemical Company and used as received. Other reagents were purchased from Aldrich, Acros or local suppliers. The compound 2,4-bis(4,4'-dimethoxybenzhydryl)-6-methylaniline was prepared using the similar procedure reported previously.¹³ The ¹H and ¹³C NMR spectroscopic measurements for the organic compounds were performed on a Bruker DMX 400 MHz and Bruker DMX 300 MHz instrument at room temperature. Chemical shifts are measured in ppm for the ¹H and ¹³C NMR spectra and are relative to TMS as an internal standard. Elemental analyses were conducted on a Flash EA 1112 microanalyzer. FT-IR spectra were recorded using a PerkinElmer System 2000 FT-IR spectrometer. The molecular weights (M_w) and molecular weight distributions (M_w/M_n) of the polyethylenes were determined using a PL-GPC220 instrument at 150 °C with 1,2,4-trichlorobenzene as the

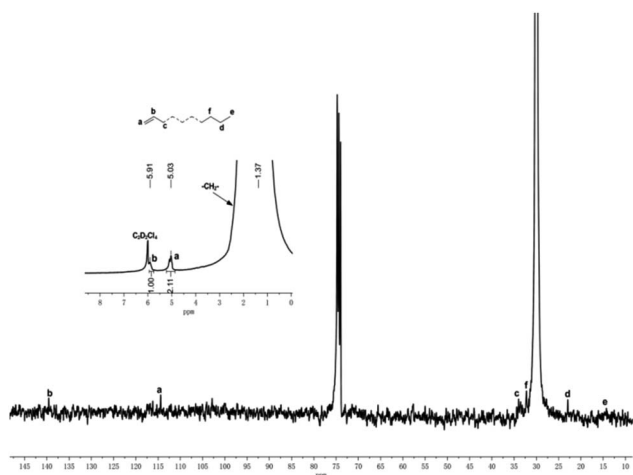


Fig. 8 The ¹H/¹³C NMR spectrum of the polyethylene produced using **Co1**/MAO (entry 6, Table 2).



solvent. The melt temperatures of the polyethylenes were measured from the second scanning run on a PerkinElmer TA-Q2000 DSC analyzer under a nitrogen atmosphere. In the procedure, a sample about 5 mg was heated to 160 °C at a heating rate of 20 °C min⁻¹ and kept for 5 min at 160 °C to remove the thermal history and then cooled at same rate to -20 °C. For the ¹H and ¹³C NMR spectra of the polyethylenes, a weighed amount of polyethylene (80–100 mg) was combined with 1,1,2,2-tetrachloroethane-*d*₂ (2 mL) with TMS as an internal standard. Inverse gated ¹³C spectra recorded on a Bruker DMX 300 spectrometer at 75.47 MHz in 5 mm standard glass tubes at 100 °C with the number of scans between 3000 and 4000. Operating conditions used: spectral width 17.9856 kHz; acquisition time 1.8219 s; relaxation delay 2 s.

Synthesis and characterization

Synthesis of 2-acetyl-6-[1-(2,4-bis(di(4-methoxyphenyl)methyl)-6-methylphenylimino)ethyl]pyridine. 1,1'-(Pyridine-2,6-diyl)bis(ethan-1-one) (3.63 g, 22.0 mmol), 2,4-bis(di(4-methoxyphenyl)methyl)-6-methylaniline (11.2 g, 20.0 mmol) and *p*-TsOH (0.68 g, 4 mmol) in toluene was stirred and heated to 120 °C for 9 h. After removing most of solvent, the residue was purified by alumina column chromatography, eluting with petroleum ether/ethyl acetate (v/v = 20 : 1) to yield as a yellow solid. (6.25 g, 44.3%). ¹H NMR (400 MHz, CDCl₃, TMS): δ 8.46 (d, *J* = 8 Hz, 1H, Py-H), 8.10 (d, *J* = 8 Hz, 1H, Py-H), 7.91 (t, *J* = 8 Hz, 1H, Py-H), 6.97 (d, *J* = 8 Hz, 4H, Ph-H), 6.88–6.78 (m, 9H, Ph-H), 6.70 (d, *J* = 8 Hz, 2H, Ph-H), 6.64 (d, *J* = 8 Hz, 2H, Ph-H), 6.57 (s, 1H, Ph-H), 5.32 (s, 1H, CH), 5.26 (s, 1H, CH), 3.79 (s, 6H, 2 × OCH₃), 3.76 (s, 3H, OCH₃), 3.73 (s, 3H, OCH₃), 2.72 (s, 3H, CH₃), 1.93 (s, 3H, CH₃), 1.63 (s, 3H, CH₃). ¹³C NMR (100 MHz, CDCl₃, TMS): δ 200.1 (C=O), 168.0 (C=N), 158.1, 157.8, 157.7, 155.6, 152.4, 146.2, 138.9, 137.3, 137.2, 137.1, 137.0, 136.0, 135.2, 135.0, 133.5, 130.5, 130.3, 130.2, 130.1, 129.2, 128.6, 124.7, 124.4, 122.4, 113.8, 113.6, 113.5, 113.3, 55.2, 54.7, 50.7, 25.6, 17.9, 16.4. FT-IR (cm⁻¹): 3001(w), 2952(w), 2902(w), 2832(w), 1698 (ν_{C=O}, m), 1638 (ν_{C=N}, w), 1606(m), 1580(w), 1508(s), 1460(m), 1444(m), 1357(w), 1298(m), 1240(s), 1174(m), 1110 (w), 1033(m), 958(w), 896(w), 813(m), 777(m), 759(w), 733(w). Anal. calcd for C₄₆H₄₄N₂O₅ (704.87): C, 78.38; H, 6.29; N, 3.97. Found: C, 78.09; H, 6.27; N, 3.89%.

Synthesis of 2-[CMeN{2,4-((4-MeOC₆H₄)₂CH)₂-6-Me}]₂-6-(CMeNAr)-C₅H₃N

L1: Ar = 2,6-Me₂C₆H₃. A suspension of 2-acetyl-6-[1-(2,4-bis(di(4-methoxyphenyl)-methyl)-6-methylphenylimino) ethyl] pyridine (1.06 g, 1.5 mmol), 2,6-dimethylaniline (0.22 g, 1.8 mmol) and *p*-TsOH (0.05 g, 0.3 mmol) in toluene was stirred and heated to 120 °C for 9 h. The resulting solution was concentrated on the rotary evaporator to give the crude reaction product, which was purified by alumina column chromatography, eluting with petroleum ether/ethyl acetate (v/v = 50 : 1) to yield as a yellow solid. (0.17 g, 14.4%). ¹H NMR (400 MHz, CDCl₃, TMS): δ 8.69 (d, *J* = 4 Hz, 1H, Py-H), 8.35 (d, *J* = 8 Hz, 1H, Py-H), 7.89 (t, *J* = 8 Hz, 1H, Py-H), 7.09 (t, *J* = 8 Hz, 2H, Ph-H), 6.98 (d, *J* = 8 Hz, 6H, Ph-H), 6.82 (m, 8H, Ph-H), 6.72 (d, *J* = 8 Hz, 2H, Ph-H), 6.66 (d, *J* = 8 Hz, 2H, Ph-H), 6.57 (s, 1H, Ph-H),

5.33 (s, 1H, CH), 5.31 (s, 1H, CH), 3.80 (s, 6H, 2 × OCH₃), 3.77 (s, 3H, OCH₃), 3.72 (s, 3H, OCH₃), 2.18 (s, 3H, CH₃), 2.09 (s, 3H, CH₃), 2.04 (s, 3H, CH₃), 1.95 (s, 3H, CH₃), 1.65 (s, 3H, CH₃). ¹³C NMR (100 MHz, CDCl₃, TMS): δ 168.7 (C=N), 167.0 (C=N), 157.9, 157.8, 155.1, 146.4, 138.8, 137.2, 137.1, 136.8, 136.2, 135.4, 133.5, 130.6, 130.3, 129.2, 128.6, 128.0, 125.5, 124.9, 123.1, 122.2, 122.1, 113.6, 113.4, 55.3, 54.8, 50.7, 18.0, 16.7, 16.5. FT-IR (cm⁻¹): 3003(w), 2950(w), 2899(w), 2833(w), 1645 (ν_{C=N}, m), 1608 (ν_{C=N}, w), 1578(m), 1508(s), 1463(m), 1449(m), 1365(w), 1299(m), 1245(s), 1209(w), 1174(m), 1120(w), 1080(w), 1036(m), 964(w), 826(w), 771(m), 750(m), 700(w). Anal. calcd for C₅₄H₅₃N₃O₄ (808.04): C, 80.27; H, 6.61; N, 5.20. Found: C, 80.02; H, 6.62; N, 5.16%.

L2: Ar = 2,6-Et₂C₆H₃. Using a similar procedure as described for L1 but with 2,6-diethylaniline as the amine, L2 was isolated as a pale yellow powder (0.29 g, 22.7%). ¹H NMR (400 MHz, CDCl₃, TMS): δ 8.43 (d, *J* = 8 Hz, 1H, Py-H), 8.34 (d, *J* = 8 Hz, 1H, Py-H), 7.88 (t, *J* = 8 Hz, 1H, Py-H), 7.11 (t, *J* = 12 Hz, 2H, Ph-H), 7.03 (t, *J* = 16 Hz, 1H, Ph-H), 6.97 (d, *J* = 8 Hz, 4H, Ph-H), 6.88 (d, *J* = 8 Hz, 2H, Ph-H), 6.83–6.77 (m, 7H, Ph-H), 6.71 (d, *J* = 8 Hz, 2H, Ph-H), 6.65 (d, *J* = 8 Hz, 2H, Ph-H), 6.56 (s, 1H, Ph-H), 5.31 (s, 1H, CH), 5.29 (s, 1H, CH), 3.79 (s, 6H, 2 × OCH₃), 3.76 (s, 3H, OCH₃), 3.71 (s, 3H, OCH₃), 2.50–2.28 (m, 4H, CH₂), 2.18 (s, 3H, CH₃), 1.94 (s, 3H, CH₃), 1.65 (s, 3H, CH₃), 1.17 (t, *J* = 16.0 Hz 3H, CH₃), 1.12 (t, *J* = 16.0 Hz 3H, CH₃). ¹³C NMR (100 MHz, CDCl₃, TMS): δ 168.7 (C=N), 167.0 (C=N), 157.9, 157.8, 155.3, 155.1, 147.9, 146.4, 138.8, 137.2, 137.1, 136.8, 136.2, 135.5, 133.5, 131.3, 131.2, 130.7, 130.3, 129.2, 128.6, 126.0, 124.9, 123.4, 122.2, 122.1, 113.6, 113.4, 55.3, 54.8, 50.7, 24.7, 24.6, 18.1, 16.8, 16.7, 13.8. FT-IR (cm⁻¹): 2296(w), 2963(w), 2935(w), 2902(w), 2832(w), 1642 (ν_{C=N}, m), 1609 (ν_{C=N}, w), 1580(m), 1508(s), 1457(m), 1418(m), 1365(w), 1300(m), 1242(s), 1174(m), 1113(w), 1075(w), 1033(m), 966(w), 872(w), 815(m), 771(m), 654(w). Anal. calcd for C₅₆H₅₇N₃O₄ (822.06): C, 80.45; H, 6.87; N, 5.03. Found: C, 80.51; H, 6.84; N, 5.05%.

L3: Ar = 2,6-*i*-Pr₂C₆H₃. Using a similar procedure as described for L1 but with 2,6-diethylaniline as the amine, L2 was isolated as a pale yellow powder (0.23 g, 26.1%). ¹H NMR (400 MHz, CDCl₃, TMS): δ 8.43 (d, *J* = 8 Hz, 1H, Py-H), 8.34 (d, *J* = 8 Hz, 1H, Py-H), 7.88 (t, *J* = 8 Hz, 1H, Py-H), 7.19–7.16 (m, 2H, Ph-H), 7.10 (t, *J* = 6 Hz, 1H, Ph-H), 6.97 (d, *J* = 8 Hz, 4H, Ph-H), 6.88 (d, *J* = 8 Hz, 2H, Ph-H), 6.84–6.77 (m, 7H, Ph-H), 6.71 (d, *J* = 8 Hz, 2H, Ph-H), 6.65 (d, *J* = 8 Hz, 2H, Ph-H), 6.56 (s, 1H, Ph-H), 5.31 (s, 1H, CH), 5.29 (s, 1H, CH), 3.79 (s, 6H, 2 × OCH₃), 3.77 (s, 3H, OCH₃), 3.71 (s, 3H, OCH₃), 2.82–2.71 (m, 2H, -CH), 2.20 (s, 3H, CH₃), 1.95 (s, 3H, CH₃), 1.67 (s, 3H, CH₃), 1.19 (d, *J* = 8 Hz, 6H, 2 × CH₃), 1.15 (d, *J* = 8 Hz, 6H, 2 × CH₃). ¹³C NMR (100 MHz, CDCl₃, TMS): δ 168.6 (C=N), 166.9 (C=N), 157.8, 157.7, 155.2, 155.0, 146.5, 146.3, 138.7, 137.1, 137.0, 136.1, 135.8, 135.4, 133.4, 130.6, 130.2, 129.1, 128.5, 124.8, 123.5, 123.0, 122.1, 122.0, 113.5, 113.3, 55.2, 54.7, 50.6, 28.3, 23.2, 22.9, 18.0, 17.1, 16.6. FT-IR (cm⁻¹): 2961(w), 2904(w), 2833(w), 1636 (ν_{C=N}, m), 1609 (ν_{C=N}, w), 1582(m), 1508(s), 1461(m), 1416(w), 1365(w), 1301(m), 1242(s), 1115(m), 1072(w), 1034(w), 967(m), 935(w), 875(w), 835(m), 816(m), 773(m), 653(w). Anal. calcd for C₅₈H₆₁N₃O₄ (864.14): C, 80.62; H, 7.12; N, 4.86. Found: C, 80.35; H, 7.11; N, 4.86%.



L4: *Ar* = 2,4,6-*Me*₃*C*₆*H*₂. Using a similar procedure as described for **L1** but with 2,4,6-trimethylaniline as the amine, **L4** was prepared as a pale yellow powder (0.29 g, 24.4%). ¹H NMR (400 MHz, CDCl₃, TMS): δ 8.43 (d, *J* = 8 Hz, 1H, Py-H), 8.34 (d, *J* = 8 Hz, 1H, Py-H), 7.88 (t, *J* = 8 Hz, 1H, Py-H), 6.97 (d, *J* = 8 Hz, 4H, Ph-H), 6.89 (d, *J* = 8 Hz, 4H, Ph-H), 6.83–6.78 (m, 7H, Ph-H), 6.71 (d, *J* = 8 Hz, 2H, Ph-H), 6.65 (d, *J* = 8 Hz, 2H, Ph-H), 6.56 (s, 1H, Ph-H), 5.31 (s, 1H, CH), 5.29 (s, 1H, CH), 3.79 (s, 6H, 2 × OCH₃), 3.76 (s, 3H, OCH₃), 3.71 (s, 3H, OCH₃), 2.30 (s, 3H, CH₃), 2.17 (s, 3H, CH₃), 2.04 (s, 3H, CH₃), 2.00 (s, 3H, CH₃), 1.94 (s, 3H, CH₃), 1.65 (s, 3H, CH₃). ¹³C NMR (100 MHz, CDCl₃, TMS): δ 168.6 (C=N), 167.4 (C=N), 157.8, 155.2, 146.4, 146.3, 138.7, 137.0, 136.7, 136.1, 135.4, 133.4, 132.2, 130.6, 130.2, 129.1, 128.6, 125.3, 125.2, 124.7, 122.1, 122.0, 113.5, 113.3, 55.2, 54.7, 50.6, 20.7, 17.9, 17.8, 16.6, 16.4. FT-IR (cm⁻¹): 2994(w), 2951(w), 2907(w), 2834(w), 1641 (ν_{C=N}, m), 1608 (ν_{C=N}, w), 1577(m), 1507(s), 1460(m), 1364(w), 1326(w), 1298(m), 1242(s), 1174(m), 1119(w), 1115(w), 1034(m), 966(w), 816(w), 779(m), 705(m), 662(w). Anal. calcd for C₅₅H₅₅N₃O₄ (822.06): C, 80.36; H, 6.74; N, 5.11. Found: C, 80.05; H, 6.80; N, 5.06%.

L5: *Ar* = 2,6-*Et*₂-4-*Me**C*₆*H*₂. Using a similar procedure as described for **L1** but with 2,6-diethyl-4-methylaniline as the amine, **L5** was prepared as a pale yellow powder (0.31 g, 25.6%). ¹H NMR (400 MHz, CDCl₃, TMS): δ 8.40 (d, *J* = 8 Hz, 1H, Py-H), 8.32 (d, *J* = 8 Hz, 1H, Py-H), 7.85 (t, *J* = 8 Hz, 1H, Py-H), 6.95 (d, *J* = 8 Hz, 6H, Ph-H), 6.86 (d, *J* = 8 Hz, 2H, Ph-H), 6.81–6.75 (m, 7H, Ph-H), 6.69 (d, *J* = 8 Hz, 2H, Ph-H), 6.63 (d, *J* = 8 Hz, 2H, Ph-H), 6.54 (s, 1H, Ph-H), 5.29 (s, 1H, CH), 5.27 (s, 1H, CH), 3.77 (s, 6H, 2 × OCH₃), 3.74 (s, 3H, OCH₃), 3.69 (s, 3H, OCH₃), 2.42–2.23 (m, 4H, CH₂), 2.34 (s, 3H, CH₃), 2.16 (s, 3H, CH₃), 1.92 (s, 3H, CH₃), 1.63 (s, 3H, CH₃), 1.14 (t, *J* = 8.0 Hz 3H, CH₃), 1.09 (t, *J* = 8.0 Hz 3H, CH₃). ¹³C NMR (100 MHz, CDCl₃, TMS): δ 168.6 (C=N), 167.1 (C=N), 157.8, 157.7, 155.2, 146.4, 145.3, 138.7, 137.1, 136.7, 136.1, 135.4, 133.4, 132.4, 131.1, 130.6, 130.2, 129.1, 128.5, 126.7, 124.9, 122.0, 113.5, 113.3, 55.2, 54.7, 50.6, 24.6, 24.5, 21.0, 17.8, 16.7, 16.6, 13.9, 13.8. FT-IR (cm⁻¹): 2994(w), 2962(w), 2904(w), 2833(w), 1641 (ν_{C=N}, m), 1607 (ν_{C=N}, w), 1577(w), 1507(s), 1459(m), 1418(w), 1364(w), 1298(m), 1244(s), 1175(m), 1116(w), 1075(w), 1034(m), 965(w), 856(w), 814(m), 775(m), 745(w). Anal. calcd for C₅₇H₅₉N₃O₄ (850.12): C, 80.53; H, 7.00; N, 4.94. Found: C, 80.16; H, 7.02; N, 4.93%.

Synthesis of [2-[CMeN{2,4-[(4-MeOC₆H₄)₂CH]₂-6-Me}]₂-6-CMe]-(CMeNAr)-C₅H₃N]CoCl₂

Co1: *Ar* = 2,6-*Me*₂*C*₆*H*₃. To a mixture of **L1** (0.202 g, 0.25 mmol) and CoCl₂ (0.031 g, 0.24 mmol) was added dichloromethane and ethanol (5/10 mL). The reaction mixture was stirred for 24 h at ambient temperature, and excess diethyl ether added to precipitate the product. The precipitate was collected by filtration, washed with diethyl ether (3 × 10 mL) and then dried under reduced pressure to give **Co1** as a brown solid (0.125 g, 56%). ¹H NMR (400 MHz, CDCl₃, TMS): δ 110.59 (s, 1H, Py-H), 108.82 (s, 1H, Py-H), 39.82 (s, 1H, Py-H), 18.23 (s, 2H, Ph-H), 9.90–8.96 (m, 16H, Ph-H), 7.55 (s, 2H, Ph-H), 5.13 (s, 6H, 2 × OCH₃), 5.08 (s, 6H, 2 × OCH₃), 4.16 (s, 3H, CH₃), 2.27 (s, 3H, CH₃), 1.84 (s, 3H, CH₃), –10.64 (s, 1H, Ph-H), –20.99 (s, 2H, 2 ×

CH), –24.59 (s, 3H, CH₃), –24.87 (s, 3H, CH₃). FT-IR (cm⁻¹): 2997(w), 2952(w), 2907(w), 2834(w), 1609 (ν_{C=N}, m), 1585 (ν_{C=N}, w), 1507(s), 1464(m), 1442(w), 1370(w), 1299(m), 1175(m), 1109(w), 1031(w), 981(m), 812(w), 771(w), 672(m). Anal. calcd for C₅₄H₅₃Cl₂CoN₃O₄ (937.87): C, 69.16; H, 5.70; N, 4.48. Found: C, 69.17; H, 5.74; N, 4.52%.

Co2: *Ar* = 2,6-*Et*₂*C*₆*H*₃. The synthesis of **Co2** was carried out using a procedure and molar ratios similar to that described for **Co1**, but with **L2** used in place of **L1**. Following work-up, **Co2** was isolated as brown powder (0.11 g, 89%). ¹H NMR (400 MHz, CDCl₃, TMS): δ 110.30 (s, 1H, Py-H), 109.34 (s, 1H, Py-H), 43.04 (s, 1H, Py-H), 19.33 (s, 2H, Ph-H), 9.90–8.96 (m, 16H, Ph-H), 8.43 (s, 2H, Ph-H), 5.26 (s, 6H, 2 × OCH₃), 5.21 (s, 6H, 2 × OCH₃), 4.49 (s, 3H, CH₃), 2.42 (s, 3H, CH₃), 1.76 (s, 3H, CH₃), –9.42 (s, 1H, Ph-H), –18.90 (s, 6H, 2 × CH₃), –20.73 (s, 4H, 2 × CH₂), –23.02 (s, 2H, 2 × CH). FT-IR (cm⁻¹): 2962(w), 2903(w), 2833(w), 1609 (ν_{C=N}, m), 1584 (ν_{C=N}, w), 1508(s), 1462(m), 1444(w), 1371(w), 1300(m), 1246(s), 1177(m), 1109(w), 1031(m), 981(w), 832(w), 811(m), 773(m), 667(w). Anal. calcd for C₅₆H₅₇Cl₂CoN₃O₄ (965.92): C, 69.63; H, 5.95; N, 4.35. Found: C, 69.48; H, 5.89; N, 4.32%.

Co3: *Ar* = 2,6-*i*-Pr₂*C*₆*H*₃. The synthesis of **Co3** was carried out using a procedure and molar ratios similar to that described for **Co1**, but with **L3** used in place of **L1**. Following work-up, **Co3** was isolated as brown powder (0.07 g, 72%). ¹H NMR (400 MHz, CDCl₃, TMS): δ 110.96 (s, 1H, Py-H), 109.53 (s, 1H, Py-H), 47.46 (s, 1H, Py-H), 19.95 (s, 2H, Ph-H), 10.01–9.44 (m, 8H, Ph-H), 6.99–6.57 (m, 8H, Ph-H), 8.43 (s, 2H, Ph-H), 5.47 (s, 6H, 2 × OCH₃), 5.26 (s, 6H, 2 × OCH₃), 3.71 (s, 3H, CH₃), 3.80 (s, 3H, CH₃), 3.16 (s, 3H, CH₃), –8.15 (s, 1H, Ph-H), –12.71 (s, 2H, 2 × CH), –13.08 (s, 6H, 2 × CH₃), –19.99 (s, 6H, 2 × CH₃), –23.16 (s, 2H, 2 × CH). FT-IR (cm⁻¹): 2960(w), 2906(w), 2873(w), 2834(w), 1609 (ν_{C=N}, m), 1584 (ν_{C=N}, w), 1508(s), 1462(m), 1444(w), 1369(w), 1300(m), 1245(s), 1175(m), 1109(w), 1031(m), 936(w), 832(w), 812(m), 771(m), 726(w). Anal. calcd for C₅₈H₆₁Cl₂CoN₃O₄ (993.98): C, 70.09; H, 6.19; N, 4.23. Found: C, 69.80; H, 6.33; N, 4.33%.

Co4: *Ar* = 2,4,6-*Me*₃*C*₆*H*₂. The synthesis of **Co4** was carried out using a procedure and molar ratios similar to that described for **Co1**, but with **L4** used in place of **L1**. Following work-up, **Co4** was isolated as brown powder (0.18 g, 71%). ¹H NMR (400 MHz, CDCl₃, TMS): δ 109.38 (s, 1H, Py-H), 109.00 (s, 1H, Py-H), 41.05 (s, 1H, Py-H), 19.76 (s, 3H, CH₃), 18.37 (s, 2H, Ph-H), 10.14–7.86 (m, 16H, Ph-H), 7.97 (s, 1H, Ph-H), 7.88 (s, 1H, Ph-H), 5.18 (s, 6H, 2 × OCH₃), 5.11 (s, 6H, 2 × OCH₃), 4.21 (s, 3H, CH₃), 2.70 (s, 3H, CH₃), 1.83 (s, 3H, CH₃), –21.48 (s, 2H, 2 × CH), –24.01 (s, 3H, CH₃), –24.23 (s, 3H, CH₃). FT-IR (cm⁻¹): 2990(w), 2905(w), 2835(w), 1610 (ν_{C=N}, m), 1585 (ν_{C=N}, w), 1509(s), 1464(m), 1444(w), 1372(w), 1300(m), 1248(s), 1178(m), 1109(w), 1033(m), 834(w), 813(w), 777(m), 672(w). Anal. calcd for C₅₅H₅₅Cl₂CoN₃O₄ (951.90): C, 69.40; H, 5.82; N, 4.41. Found: C, 69.45; H, 5.84; N, 4.44%.

Co5: *Ar* = 2,6-*Et*₂-4-*Me**C*₆*H*₂. The synthesis of **Co5** was carried out using a procedure and molar ratios similar to that described for **Co1**, but with **L5** used in place of **L1**. Following work-up, **Co5** was isolated as brown powder (0.10 g, 80%). ¹H NMR (400 MHz, CDCl₃, TMS): δ 109.14 (s, 2H, Py-H), 44.09 (s, 1H, Py-H), 20.26 (s,



3H, CH₃), 18.91 (S, 2H, Ph-H), 10.75–9.06 (m, 16H, Ph-H), 8.41 (S, 2H, Ph-H), 5.25 (S, 6H, 2 × OCH₃), 5.21 (S, 6H, 2 × OCH₃), 4.48 (S, 3H, CH₃), 2.32 (S, 3H, CH₃), 1.68 (S, 3H, CH₃), –19.05 (S, 6H, 2 × CH₃), –21.11 (S, 4H, 2 × CH₂), –22.08 (S, 2H, 2 × CH). FT-IR (cm⁻¹): 2980(w), 2902(w), 2833(w), 1609 ($\nu_{C=N}$, m), 1584 ($\nu_{C=N}$, w), 1508 (s), 1461(m), 1411(w), 1374(w), 1300(m), 1248(s), 1177(m), 837(w), 813(m), 777(m), 674(w). Anal. calcd for C₅₇H₅₉Cl₂CoN₃O₄ (979.95): C, 69.86; H, 6.07; N, 4.29. Found: C, 69.87; H, 6.07; N, 4.34%.

X-ray crystallographic studies

The single-crystals diffraction studies for **Co2** and **Co4** were performed using a Rigaku Sealed Tube CCD (Saturn 724+) diffractometer with graphite-monochromated Cu-K α radiation ($\lambda = 1.54184 \text{ \AA}$) at 173(2) K. Cell parameters were obtained by global refinement of the positions of all collected reflections. Intensities were corrected for Lorentz and polarization effects and empirical absorption. The structures were solved by direct methods and refined by full matrix least squares on F^2 . All hydrogen atoms were placed in calculated positions. Structure solution and refinement were performed by using the SHELXL-97 package. Crystal data and structure refinements for **Co2** and **Co4** are shown in Table S4.[†] CCDC 2027357 and 2027358 contain the supplementary crystallographic data for complexes **Co2** and **Co4**, respectively.[†]

Polymerization studies

Ethylene polymerization at 1 atm C₂H₄. Precatalyst **Co1** (1.4 mg, 1.5 μmol) was added to a Schlenk vessel with a magnet stir bar followed by freshly distilled toluene (30 mL) and then the required amount of aluminum activator (MAO, MMAO) was introduced *via* syringe. The solution was afterwards stirred at 50 °C under 1 atm of C₂H₄ introduced by a rubber gas bag. After 30 min, the pressure was vented and the reaction quenched with acidified ethanol (ethanol/HCl = 50/1). The suspension was stirred for 1 h, after that the precipitated polymer was washed with ethanol, dried under vacuum at 50 °C and then weighed.

Ethylene polymerization at 5/10 atm C₂H₄. The polymerization at high ethylene pressure was carried out in a stainless-steel autoclave (250 mL) equipped with an ethylene pressure controller, a mechanical agitator and a thermoregulatory. At the desired reaction temperature the precatalyst (**Co1–Co5**: 1.5 μmol) dissolved in toluene (50 mL) was injected into the autoclave, followed by freshly distilled toluene (25 mL). The required amount of aluminum activator like MAO, MMAO, and more toluene (25 mL) were then injected successively to complete the addition. With rapid stirring, the autoclave was immediately pressurized to the setting ethylene pressure (5/10 atm). After a prescribed reaction time, the ethylene pressure was vented and the reaction quenched with acidified ethanol (ethanol/HCl = 50/1). The suspension was stirred for 1 h, and then the precipitated polymer was filtered and washed with anhydrous ethanol and dried under vacuum at 50 °C and weighed.

Conclusions

A series of unsymmetrical 2-(2,4-bis(di(4-methoxyphenyl)methyl)-6-MeC₆H₂N)-6-(1-(arylimino)ethyl)pyridine cobalt complexes has been synthesized and fully characterized. The molecular structures of the representative cobalt complexes **Co2** and **Co4** were obtained by the single-crystal X-ray diffraction method, showing distorted square-pyramidal geometry at the metal. Activated with either MAO or MMAO, all precatalysts **Co1–Co5** displayed high activities towards ethylene polymerization, especially when using **Co1**/MAO (Al/Co = 3250 at 50 °C under 10 atm ethylene), up to $9.17 \times 10^6 \text{ g PE (mol of Co)}^{-1} \text{ h}^{-1}$) producing strictly linear polyethylene with high molecular weight ($3.14 \times 10^5 \text{ g mol}^{-1}$) and wide polydispersity (54.6). In particular, regardless of whether Co/MAO or Co/MMAO catalytic system, ethylene undergoes β -hydride elimination reaction pathway during polymerization, resulting in vinyl-polyethylene. Therefore, the introduction of methoxy to the benzhydryl group results in a significant increase in the molecular weight of the produced polyethylene as well as the wide polydispersities (around 50), the first time obtaining the high-density polyethylene with wide polydispersity similar to ones produced by chromium Phillips catalysis.¹⁰ The less toxic cobalt catalysts potentially replace Phillips catalysts in commercial application for the polydispersive polyethylenes.

Conflicts of interest

There are no conflicts to declare.

Acknowledgements

This work was supported by the National Natural Science Foundation of China (No. 21871275).

Notes and references

- (a) G. J. P. Britovsek, V. C. Gibson, B. S. Kimberley, P. J. Maddox, S. J. McTavish, G. A. Solan, A. J. P. White and D. J. Williams, *Chem. Commun.*, 1998, 7, 849–850; (b) B. L. Small, M. Brookhart and A. M. A. Bennett, *J. Am. Chem. Soc.*, 1998, **120**, 4049–4050; (c) G. J. P. Britovsek, M. Bruce, V. C. Gibson, B. S. Kimberley, P. J. Maddox, S. Mastroianni, S. J. McTavish, C. Redshaw, G. A. Solan, S. Strömberg, A. J. P. White and D. J. Williams, *J. Am. Chem. Soc.*, 1999, **121**, 8728–8740.
- (a) Z. Flisak and W.-H. Sun, *ACS Catal.*, 2015, **5**, 4713–4724; (b) Z. Wang, G. A. Solan, W. Zhang and W.-H. Sun, *Coord. Chem. Rev.*, 2018, **363**, 92–108; (c) C. Bariashir, C. Huang, G. A. Solan and W.-H. Sun, *Coord. Chem. Rev.*, 2019, **385**, 208–229; (d) S. Yuan, Y. Yan, G. A. Solan, Y. Ma and W.-H. Sun, *Coord. Chem. Rev.*, 2020, **411**, 213254.
- (a) W.-H. Sun, P. Hao, S. Zhang, Q. Shi, W. Zuo, X. Tang and X. Lu, *Organometallics*, 2007, **26**, 2720–2734; (b) Y. Chen, P. Hao, W. Zuo, K. Gao and W.-H. Sun, *J. Organomet. Chem.*, 2008, **693**, 1829–1840; (c) R. Gao, Y. Li, F. Wang, W.-H. Sun and M. Bochmann, *Eur. J. Inorg. Chem.*, 2009,



- 4149–4156; (d) L. Xiao, R. Gao, M. Zhang, Y. Li, X. Cao and W.-H. Sun, *Organometallics*, 2009, **28**, 2225–2233; (e) W. Lin, L. Zhang, J. Gao, Q. Zhang, Y. Ma, H. Liu and W.-H. Sun, *Molecules*, 2020, **25**, 4244; (f) W. Lin, L. Zhang, H. Suo, A. Vignesh, N. Yousuf, X. Hao and W.-H. Sun, *New J. Chem.*, 2020, **44**, 8076–8084.
- 4 K. Wang, K. Wedeking, W. Zuo, D. Zhang and W.-H. Sun, *J. Organomet. Chem.*, 2008, **693**, 1073–1080.
- 5 S. Zhang, W.-H. Sun, T. Xiao and X. Hao, *Organometallics*, 2010, **29**, 1168–1173.
- 6 (a) J. D. A. Pelletier, Y. D. M. Champouret, J. Cadarso, L. Clowes, M. Gañete, K. Singh, V. Thanarajasingham and G. A. Solan, *J. Organomet. Chem.*, 2006, **691**, 4114–4123; (b) S. Jie, S. Zhang, K. Wedeking, W. Zhang, H. Ma, X. Lu, Y. Deng and W.-H. Sun, *C. R. Chim.*, 2006, **9**, 1500–1509; (c) S. Jie, S. Zhang and W.-H. Sun, *Eur. J. Inorg. Chem.*, 2007, 5584–5598; (d) M. Zhang, R. Gao, X. Hao and W.-H. Sun, *J. Organomet. Chem.*, 2008, **693**, 3867–3877; (e) J. Guo, W. Zhang, T. Liang and W.-H. Sun, *Polyhedron*, 2020, **193**, 114865.
- 7 (a) W. Zhang, W.-H. Sun and C. Redshaw, *Dalton Trans.*, 2013, **42**, 8988–8997; (b) B. Gansukh, R. Zhang, J. Guo, W. Zhang and W.-H. Sun, *Gen. Chem.*, 2020, **6**, 190031–190039.
- 8 (a) S. Jie, W.-H. Sun and T. Xiao, *Chin. J. Polym. Sci.*, 2010, **28**, 299–304; (b) T. Xiao, W. Zhang, J. Lai and W.-H. Sun, *C. R. Chim.*, 2011, **14**, 851–855; (c) Z. Wang, G. A. Solan, Y. Ma, Q. Liu, T. Liang and W.-H. Sun, *Research*, 2019, **2019**, 1–15; (d) C. Bariashir, Z. Wang, Y. Ma, A. Vignesh, X. Hao and W.-H. Sun, *Organometallics*, 2019, **38**, 4455–4470; (e) J. Guo, W. Zhang, I. I. Oleynik, G. A. Solan, I. V. Oleynik, T. Liang and W.-H. Sun, *Dalton Trans.*, 2020, **49**, 136–146; (f) M. Han, Q. Zhang, I. I. Oleynik, H. Suo, G. A. Solan, I. V. Oleynik, Y. Ma, T. Liang and W.-H. Sun, *Dalton Trans.*, 2020, **49**, 4774–4784.
- 9 (a) J. Ba, S. Du, E. Yue, X. Hu, Z. Flisak and W.-H. Sun, *RSC Adv.*, 2015, **5**, 32720–32729; (b) V. K. Appukuttan, Y. Liu, B. C. Son, C.-S. Ha, H. Suh and I. Kim, *Organometallics*, 2011, **30**, 2285–2294; (c) W.-H. Sun, S. Kong, W. Chai, T. Shiono, C. Redshaw, X. Hu, C. Guo and X. Hao, *Appl. Catal. Gen.*, 2012, **447–448**, 67–73; (d) F. Huang, W. Zhang, E. Yue, T. Liang, X. Hu and W.-H. Sun, *Dalton Trans.*, 2016, **45**, 657–666; (e) S. Du, W. Zhang, E. Yue, F. Huang, T. Liang and W.-H. Sun, *Eur. J. Inorg. Chem.*, 2016, 1748–1755; (f) Z. Wang, G. A. Solan, Q. Mahmood, Q. Liu, Y. Ma, X. Hao and W.-H. Sun, *Organometallics*, 2018, **37**, 380–389; (g) Q. Zhang, N. Wu, J. Xiang, G. A. Solan, H. Suo, Y. Ma, T. Liang and W.-H. Sun, *Dalton Trans.*, 2020, **49**, 9425–9437; (h) Q. Zhang, R. Zhang, M. Han, W. Yang, T. Liang and W.-H. Sun, *Dalton Trans.*, 2020, **49**, 7384–7396.
- 10 P. M. Max, *Adv. Catal.*, 2010, **53**, 123–606.
- 11 (a) S. Wang, B. Li, T. Liang, C. Redshaw, Y. Li and W.-H. Sun, *Dalton Trans.*, 2013, **42**, 9188–9197; (b) F. He, W. Zhao, X.-P. Cao, T. Liang, C. Redshaw and W.-H. Sun, *J. Organomet. Chem.*, 2012, **713**, 209–216; (c) Q. Mahmood, Y. Ma, X. Hao and W.-H. Sun, *Appl. Organomet. Chem.*, 2019, **33**, e4857; (d) R. Zhang, Y. Ma, M. Han, G. A. Solan, Y. Pi, Y. Sun and W.-H. Sun, *Appl. Organomet. Chem.*, 2019, **33**, e5175; (e) L. Guo, H. Gao, L. Zhang, F. Zhu and Q. Wu, *Organometallics*, 2010, **29**, 2118–2125; (f) W. Zhao, E. Yue, X. Wang, W. Yang, Y. Chen, X. Hao, X. Cao and W.-H. Sun, *J. Polym. Sci., Part A: Polym. Chem.*, 2017, **55**, 988–996; (g) A. S. Ionkin, W. J. Marshall, D. J. Adelman, B. B. Fones, B. M. Fish and M. F. Schifffauer, *Organometallics*, 2008, **27**, 1902–1911; (h) R. Zhang, M. Han, Y. Ma, G. A. Solan, T. Liang and W.-H. Sun, *Dalton Trans.*, 2019, **48**, 17488–17498.
- 12 (a) J. Yu, W. Huang, L. Wang, C. Redshaw and W.-H. Sun, *Dalton Trans.*, 2011, **40**, 10209–10214; (b) S. Wang, W. Zhao, X. Hao, B. Li, C. Redshaw, Y. Li and W.-H. Sun, *J. Organomet. Chem.*, 2013, **731**, 78–84; (c) J. Lai, W. Zhao, W. Yang, C. Redshaw, T. Liang, Y. Liu and W.-H. Sun, *Polym. Chem.*, 2012, **3**, 787; (d) W. Zhang, S. Wang, S. Du, C.-Y. Guo, X. Hao and W.-H. Sun, *Macromol. Chem. Phys.*, 2014, **215**, 1797–1809; (e) S. Du, S. Kong, Q. Shi, J. Mao, C. Guo, J. Yi, T. Liang and W.-H. Sun, *Organometallics*, 2015, **34**, 582–590.
- 13 (a) S. Meiries, K. Speck, D. B. Cordes, A. M. Z. Slawin and S. P. Nolan, *Organometallics*, 2012, **32**, 330–339; (b) S.-F. Yuan, Z. Fan, Q. Zhang, Z. Flisak, Y. Ma, Y. Sun and W.-H. Sun, *Appl. Organomet. Chem.*, 2020, **34**, e5638.
- 14 (a) G. J. P. Britovsek, V. C. Gibson, B. S. Kimberley, S. Mastroianni, C. Redshaw, G. A. Solan, A. J. P. White and D. J. Williams, *J. Chem. Soc., Dalton Trans.*, 2001, **10**, 1639–1644; (b) Q. Zhang, Y. Ma, H. Suo, G. A. Solan, T. Liang and W.-H. Sun, *Appl. Organomet. Chem.*, 2019, **33**, e5134; (c) Z. Wang, Y. Ma, J. Guo, Q. Liu, G. A. Solan, T. Liang and W.-H. Sun, *Dalton Trans.*, 2019, **48**, 2582–2591; (d) H. Suo, Z. Li, I. V. Oleynik, Z. Wang, I. I. Oleynik, Y. Ma, Q. Liu and W.-H. Sun, *Appl. Organomet. Chem.*, 2020, **34**, e5937.
- 15 (a) F. Huang, W. Zhang, Y. Sun, X. Hu, G. A. Solan and W.-H. Sun, *New J. Chem.*, 2016, **40**, 8012–8023; (b) H. Suo, I. I. Oleynik, C. Bariashir, I. V. Oleynik, Z. Wang, G. A. Solan, Y. Ma, T. Liang and W.-H. Sun, *Polymer*, 2018, **149**, 45–54; (c) J. Guo, Z. Wang, W. Zhang, I. I. Oleynik, A. Vignesh, I. V. Oleynik, X. Hu, Y. Sun and W.-H. Sun, *Molecules*, 2019, **24**, 1176; (d) C. Bariashir, Z. Wang, H. Suo, M. Zada, G. A. Solan, Y. Ma, T. Liang and W.-H. Sun, *Eur. Polym. J.*, 2019, **110**, 240–251; (e) Y. Huang, R. Zhang, T. Liang, X. Hu, G. A. Solan and W.-H. Sun, *Organometallics*, 2019, **38**, 1143–1150; (f) M. Zada, A. Vignesh, H. Suo, Y. Ma, H. Liu and W.-H. Sun, *Mol. Catal.*, 2020, **492**, 110981; (g) M. Han, Q. Zhang, I. I. Oleynik, H. Suo, I. V. Oleynik, G. Solan, Y. Ma, T. Liang and W.-H. Sun, *Catalysts*, 2020, **10**, 1002.
- 16 S. Du, X. Wang, W. Zhang, Z. Flisak, Y. Sun and W.-H. Sun, *Polym. Chem.*, 2016, **7**, 4188–4197.
- 17 (a) Z. Long, B. Wu, P. Yang, G. Li, Y. Liu and X.-J. Yang, *J. Organomet. Chem.*, 2009, **694**, 3793–3799; (b) C. Huang, S. Du, G. A. Solan, Y. Sun and W.-H. Sun, *Dalton Trans.*, 2017, **46**, 6948–6957.
- 18 Q. Mahmood, E. Yue, J. Guo, W. Zhang, Y. Ma, X. Hao and W.-H. Sun, *Polymer*, 2018, **159**, 124–137.



Paper

- 19 (a) W. Zhao, J. Yu, S. Song, W. Yang, H. Liu, X. Hao, C. Redshaw and W.-H. Sun, *Polymer*, 2012, **53**, 130–137; (b) X. Cao, F. He, W. Zhao, Z. Cai, X. Hao, T. Shiono, C. Redshaw and W.-H. Sun, *Polymer*, 2012, **53**, 1870–1880.
- 20 (a) L. Guo, M. Zada, W. Zhang, A. Vignesh, D. Zhu, Y. Ma, T. Liang and W.-H. Sun, *Dalton Trans.*, 2019, **48**, 5604–5613; (b) M. Zada, L. Guo, Y. Ma, W. Zhang, Z. Flisak, Y. Sun and W.-H. Sun, *Molecules*, 2019, **24**, 2007; (c) R. Zhang, Y. Huang, G. A. Solan, W. Zhang, X. Hu, X. Hao and W.-H. Sun, *Dalton Trans.*, 2019, **48**, 8175–8185.
- 21 (a) G. M. Sheldrick, *Acta Crystallogr., Sect. C: Struct. Chem.*, 2015, **71**, 3–8; (b) G. M. Sheldrick, *Acta Crystallogr., Sect. A: Found. Adv.*, 2015, **71**, 3–8.

